Supporting information for

Covalent Surface Functionalization of Carbon Nitrides: A Case Study of Poly(Heptazine Imide)

Florian Binder,[a,b] Igor Moudrakovski,[a] Nils L. Kötter,[b] Saunak Das,[a] Kathrin Küster,[a] Sebastian Bette[a] and Bettina V. Lotsch*[a,b]

[a] Max Planck Institute for Solid State Research, Heisenbergstr. 1, 70569 Stuttgart, Germany

E-mail: b.lotsch@fkf.mpg.de

[b] Department of Chemistry, University of Munich, LMU, Butenandtstr. 5-13, 81377 Munich, Germany

*corresponding author:

b.lotsch@fkf.mpg.de

Table of Contents

1. Instrumental details

The analysis by powder X-ray diffraction (PXRD) was performed on a Stoe Stadi P-diffractometer (Cu-$K_{\alpha 1}$ radiation, λ = 1.5406 Å) at room temperature. A Mythen 1K Stoe detector with Debye-Scherrer geometry and a Ge(111) monochromator were used. The grounded samples were sealed in Hilgenberg glass capillaries (No.014) with 0.3 mm diameter. The diffraction was recorded in a range from 2.000 to 62.735°, using a step size of 0.015° with a total acquisition time of 72 minutes.

Fourier transformed infrared (FT-IR) spectra were measured on a Jasco FT/IR-4600 device with an ATR diamond unit.

C, H, N, S elemental combustion analysis (EA) was conducted on an elemental analyzer by Vario El with helium as carrier gas. Other elements were quantified by inductively coupled plasma optical emission spectrometry (ICP-OES). Samples were measured on a Varian Vista RL spectrometer.

^{19}F liquid nuclear magnetic resonance spectra (NMR) were measured at 298 K on a Varian Mercur 200 or on a Joel Eclipse 270 MHz and 400 MHz device at the LMU of Munich. Solid-state nuclear magnetic resonance (ssNMR) experiments were performed on a Bruker Avance-III 400 MHz and Neo 600 MHz wide bore instruments (magnetic fields B0 of 9.4 T and 14.1 T, respectively) with magic angle spinning (MAS) rates ranging between 8 and 60 kHz. The nuclei ^{1}H, ^{13}C, ^{15}N and ^{19}F were measured at frequencies of 400, 100.61, 40.53, 376.3 MHz (B0 = 9.4 T) and 600.3, 150.85, 60.8, 564.8 MHz (B0 = 14.1 T), respectively. External chemical shift references were tetramethylsilane (TMS, δ(^{1}H, ^{13}C) = 0.0 ppm), nitromethane (δ(^{15}N) = 0.0 ppm) and teflon (δ(^{19}F) = -123.2 ppm)[1,2]. ^{15}N and ^{13}C Cross-Polarization (CP) spectra were recorded using a ramped-amplitude polarization transfer[3] followed by Spinal-64 proton decoupling (^{1}H RF field of 50 kHz)[4]. For ^{19}F quantitative ssNMR measurements, a defined amount of CaF_2 was thoroughly mixed to a defined amount of the sample. From the resulting integrals, the amount of surface functionalization was calculated. For the screening experiments of different bases and temperatures, the integrals from CaF_2 were divided by 0.82 to correct on incomplete relaxation of the reference. Double Cross- Polarization technique employed in ^{15}N-^{13}C 2D NMR heteronuclear correlation experiments uses two consecutive cross polarization steps. The first step transfers polarization from protons to ^{15}N, the second step transfers the resulting polarization to ^{13}C in order to probe the dipolar coupling between these two nuclei[5,6]. The 2D NMR measurements performed at a rotation frequency of 11 or 12 kHz and optimized contact times in the consecutive polarization steps of 1 and 2 ms. 1D ^{13}C and ^{15}N measurements usually had 3 ms of contact time, but the ^{13}C reference K-PHI had a contact time of 2 ms. The number of accumulations and relaxation delay are optimized as well, and are 16 and 2–4 s for ^{1}H, 2000–40000 and 1–2.5 s for ^{13}C, 80000 and 1–2 s for ^{15}N, about 300 and 250 s for ^{19}F and 720–800 and 1–1.2 s for 2D measurements, respectively.

For ultraviolet-visible (UV-Vis) spectroscopy, an Jasco V-650 spectrophometer was used. The optical band gap was estimated by using the reflectance spectra in percentage, converting them

using the Kubelka Munk function and plotting the data in a Tauc plot under the assumption of a direct optical band gap.

Morphology and additional chemical composition investigations were examined by scanning electron microscopy (SEM; Merlin, Zeiss) and SEM energy dispersive X-ray spectroscopy (SEM-EDX) using a Si/Li detector (Ultim Extreme, Oxford). Transmission electron microscopy (TEM) data were collected with a Philips CM 30 ST microscope (300 kV, LaB_6 cathode). The sample was suspended in butanol and distributed onto a holey carbon/copper grid. Images were taken with a TVIPS TemCam-F216 CMOS Camera. The program EM-Menu 4.0 Extended was used to perform TEM-fast Fourier Transform (TEM-FFT).

Zeta-potential was determined with a Zetasizer Nano ZS (Malvern Instruments) with a 4 mW He-Ne laser (633 nm) using electrophoretic light scattering. The samples were prepared by sonicating 1 mg of the material in 10 mL of a 10 mM NaCl solution.

X-ray photoelectron spectroscopy (XPS) data were acquired on powder samples, which were pressed into Indium foils. An Axis Ultra (Kratos Analytical, Manchester) equipped with an Al Kα X-ray monochromatic source. The charge neutralization was used for charge compensation and the the binding energies were calibrated against the adventitious C 1s spectral signature at 284.8 eV.[7] The raw data were fitted with a LA-line shape after Shirley background subtraction using the CasaXPS 2.3.26rev1 software.[8] The binding energies were compared with respect to the standard NIST Reference Database 20 (Version 4.1), unless specified. The relative transmission functions and sensitivity factors given by the instrument manufacturer were utilized to quantify the recorded spectra to deduce respective material compositions.

Static contact angles of millipore water were measured on 6 mm thick freshly prepared carbon nitride pellets (pressed at 2 bar) using an Ossila BV Contact Angle Goniometer. Measurements were done under ambient conditions with three concurrent measurements on different pellets to determine the average angles. The water droplet was prepared using a fine Hamilton microliter syringe (600 series) tip and a constant drop volume (1.5 µl) was maintained for each case which was released from a fixed height, and imaged after 10 seconds of equilibration time. The data was processed using Ossila's automatic edge detection tool and verified by manual reconstruction of angles by a protractor. Finally, the average values with standard deviations are reported.

For thermogravimetric analysis (TGA) measurement, samples were put in an alumina crucible. Measurements were then carried out using a Netzsch, STA 449 F5 Jupiter with Argon flow in a temperature range between 20 °C and 700 °C and heating rates of 10 K/min. Data handling was performed with the Netzsch Proteus software package.

Mass spectrometry samples were prepared by solving the sample in a mixture of acetonitrile and water. Electrospray ionization (ESI) was used as a method. The measurement was carried out with a Thermo Finnigan LTQ FT Ultra Fourier Transform ionic Cyclotron resonance mass spectrometer with a resolution of 100000 at m/z 400. The voltage of the spray capillaries at the IonMax ESI-head was 4 kV, the temperature of the heat capillaries was 250 °C and the nitrogen sheath gas flow was 20 units, while the sweep gas flow was five units.

For purification of samples, mostly centrifugation, carried out with a benchtop centrifuge Sigma-3-30 K from Sigma, was used. Sonication was performed using an ultrasonic bath Elmasonic S 100 with a high-performance 37 kHz sandwich transducer system and state-of-the art microprocessor controlled ultrasonic cleaning and sweeping technology.

2. Experimental details

2.1. Materials and reagents

All reagents, materials and solvents were used as received from commercial suppliers without further purification. Melon,[9] protonated poly(heptazine imide) (H-PHI),[9] different sized potassium poly(heptazine imide) (K-PHI),[10] melamine functionalized PHI (Mel-PHI),[11] poly(triazine imide) (PTI),[12] melem[13] and melem oligomers[14] were synthesized as described in literature with their characterizations being in agreement with the reported ones.

2.2. Functionalization

Carbon nitride functionalization was conducted similar to a typical amide synthesis using acyl chlorides.[15] The general procedure used for carbon nitrides is given in the following. To optimize the conditions and compare between carbon nitrides, usually only one parameter was changed. An overview about synthetic optimization and different carbon nitride functionalizations is given in table S1.

Generally, K-PHI (200 mg) was dried in a sealed microwave vessel under high vacuum and heat. After purging with argon, tetrahydrofuran (THF, dry, 4.0 mL, Acros organics, ≥ 99.5 %), 4-(trifluoromethyl)benzoyl chloride (0.30 mL, 2.02 mmol, Fisher scientific, ≥ 97 %) and triethylamine (0.69 mL, 4.97 mmol, Acros organics, ≥ 99 %) were added. The reaction mixture was stirred at 70 °C for 17 h. The crude product was purified by centrifuging four times with THF (VWR chemicals, ≥ 99 %) (16 k rpm, 15 min, 15 °C) and three times with deionized (DI) water (22 k rpm, 10 min, 15 °C), followed by drying at 60 °C over night.

Table S1. Variations of the general K-PHI functionalization routine and comparison with other carbon nitrides. The functionalization degree is given by the ratio between functionalized heptazine units divided by overall heptazine units. It is calculated from quantitative ^{19}F ssNMR measurements. Mark that a functionalization degree of 100 % is not possible for a 2D carbon nitride. When the changed condition is sonication, this means that the reaction mixtures were sonicated for 0.5 h right before heating the mixture under stirring. For the standard conditions and for a reaction time of 1 h, three experiments were conducted, respectively. The deviation is expected to result from variations in surface groups and particle size of different K-PHI batches, while the age of the acyl chloride might also influence the reaction.

Changed condition	Value	Yield (FG per heptazine ratio) [%]
Nothing		0.94 ± 0.47
Temperature	25 °C	0.54
Base	K_3PO_4	0.37
	NaOH	0.50
Base, temperature	K_3PO_4, 25 °C	0.11
	NaOH, 25 °C	0.32
Carbon nitride	H-PHI	0.97
	Mel-PHI	1.70
	Melon	0.71
	PTI	0.98*
	Melem oligomers	1.14
	Melem	262.5
	Melamine	300*
Particle size	400–650 nm	1.29
	200–400 nm	2.19
	150–250 nm	2.41
Reaction time	0.5 h	1.86
	1 h	1.5 ± 0.62
	2 h	3.26
	6 h	2.28
	41 h	0.56
Sonication, carbon nitride	Melon	2.64
	H-PHI	1.29
	Mel-PHI	1.68
	Melem oligomers	2.86
Optimized conditions	See section 2.3.	12.48

*For PTI and melamine, the functionalization degree is given for triazine units instead of heptazine units.

2.3. Optimized functionalization for PHI

For the optimized functionalization of PHI, H-PHI particles with a size of about 200 nm were used. H-PHI (123 mg) was dried in a sealed microwave vessel by heating under high vacuum. The vessel was purged with argon, followed by adding tetrahydrofuran (THF, dry, 2.5 mL), 4-(trifluoromethyl)benzoyl chloride (0.18 mL, 1.24 mmol) and triethylamine (0.43 mL,

3.05 mmol. The reaction mixture was sonicated for 30 min and stirred at 70 °C for 2 h afterwards. The crude product was centrifuged four times with THF (16 k rpm, 15 min, 15 °C) and three times with deionized (DI) water (22 k rpm, 10 min, 15 °C) and dried at 60 °C over night.

2.4. ^{15}N K-PHI

^{15}N enriched K-PHI was prepared in a two-step synthesis. First, ground ^{15}N enriched urea (3.00 g, 48.3 mmol, Sigma-Aldrich, ≥ 98 %) was given in an ampoule, equipped with a quick fit and a tube that was put into a vessel with water. The ampoule was heated to 600 °C with a heating rate of 15 K/min and the temperature was kept for 2 h. The resulting mixture of polymeric and small carbon nitrides was washed with water. The residue (0.982 mg) was mixed with potassium iodide (3.76 g, 22.7 mmol, Sigma-Aldrich, ≥ 99 %). After grinding, the resulting reaction mixture was put again in an ampoule equipped with a quick fit and a tube that was in a water vessel. The ampoule was heated to 525 °C for 2 h with a heating rate of 15 K/min. The crude product was washed four times by centrifugation with water (22 k rpm, 15 min, 15 °C). After drying at 60 °C over night, yellow ^{15}N-enriched K-PHI (0.208 g) was obtained.

2.5. ^{13}C enriched functional group

2.5.1. Benzoic acid-α-^{13}C

Benzoic acid-α-^{13}C was synthesized similar to a synthesis by S. Shibata *et al.*[16] In a three-neck round-bottom flasks, a phenylmagnesium bromide solution (45 mL, 1 M, 45.0 mmol, 1.0 eq., Sigma-Aldrich) was diluted with anhydrous THF (45 mL). The mixture was frozen using liquid nitrogen. Vacuum was applied and $^{13}CO_2$ (1 L STP, 45 mmol, 99 atom% ^{13}C, Sigma-Aldrich, ≥ 99 %) was slowly resublimed into the flask. The reaction mixture was allowed to warm to -78 °C in an atmosphere of argon (1 bar). The grey reaction mixture was stirred at -78°C for 30 min and was then allowed to slowly warm to -20 °C over 2 h. The reaction was quenched through addition of NaOH (6 M, 50 mL) and extracted with dichlormethane (2 x 100 mL, Acros organics, ≥ 99.99 %). The organic layer was extracted with water (pH >7, 2x75 mL). The combined aqueous layers were acidified with dilute HCl and extracted with DCM (3 x 150 mL). The solvent was removed and the residual white solid dried under high vacuum to yield benzoic acid-α-^{13}C (4.07 g, 33.1 mmol, 73%) as a white solid. ^{1}H NMR (400 MHz, $CDCl_3$) δ 8.25 – 8.03 (m, 2H), 7.68 – 7.58 (m, 1H), 7.54 – 7.42 (m, 2H). ^{13}C NMR (101 MHz, $CDCl_3$) δ 172.2 (COOH), 134.0 (d, J_{CC} = 1.1 Hz, *p*-C), 130.4 (d, J_{CC} = 2.7 Hz, *o*-C), 129.4 (d, J_{CC} = 72.5 Hz, *i*-C), 128.6 (d, J_{CC} = 4.5 Hz, *m*-C). HRMS (ESI-): m/z calc. for $C_6{}^{13}CH_5O_2^-$ (M^-): 122.03286; found: 122.03277.

2.5.2. Benzoyl chloride-α-^{13}C

The synthesis was conducted according to a procedure of J. A. Kepler *et al.*[17] In a two-neck round-bottom flask, benzoic acid-α-^{13}C (1.85 g, 15.0 mmol, 1.0 eq.) was suspended in anhydrous benzene (10 mL, Sigma-Aldrich, ≥ 99.5 %). Thionyl chloride (2.8 mL, 38.4 mmol, 2.6 eq., Fisher scientific, ≥ 99.5 %) was added and the reaction mixture was heated to 75 °C for 4 h, followed by refluxing at 105 °C for 1 h. The reaction was cooled to room temperature and residual thionyl chloride and solvent were removed under reduced pressure. The residual liquid was purified by distillation under reduced pressure (75 °C, <10 mbar) to yield benzoyl chloride-α-^{13}C (1.65 g, 11.7 mmol, 78%) as a clear liquid. ^{1}H NMR (400 MHz, $CDCl_3$) δ 8.07 – 7.95 (m, 2H), 7.66 – 7.54 (m, 1H), 7.49 – 7.37 (m, 2H). ^{13}C NMR (101 MHz, $CDCl_3$) δ 168.5 (COCl), 135.4 (d, J_{CC} = 1.2 Hz, *p*-C), 133.3 (d, J_{CC} = 74.2 Hz, *i*-C), 131.5 (d, J_{CC} = 3.1 Hz, *o*-C), 129.1 (d, J_{CC} = 5.4 Hz, *m*-C).

3. Additional information

3.1. Tables

Table S2. Literature yields for organic surface functionalizations on carbon nitrides. Only literature where functionalization was investigated quantitatively is shown. From these quantifications, the functional group (FG) per heptazine ratio was calculated. Mark that unreacted group removal might not be investigated sufficiently, which could influence the covalent yield. All shown functionalizations were conducted on melon based polymeric carbon nitrides.

Publication year	Functional group	Yield (FG per heptazine ratio) [%]	Reference
2016	Zinc tetracarboxyphthalocyanine	0.57	24
2016	Perylene tetracarboxylic dianhydride	2.38	25
2017	Ferrocene	5.00	26
2020	Nickel bis-aminothiophenol	0.47	27
2020	Cobalt quaterpyridine	0.03	22
2022	Iron quaterpyridine	0.06	28

Table S3. XPS results compared to K-PHI in of functionalized PHI atom %.

Element	K-PHI [at. %]	PHI funct. [at. %]
N	48.4	48.8
C	44.0	49.1
O	3.2	1.4
F	-	0.6
K	4.2	-
C/N ratio	0.9091	1.0061

Table S4. EA results are shown. The functionalized H-PHI is compared to H-PHI. Atomic % were calculated by comparing the C/N ratios, assuming that the higher carbon content only belongs to the FG, calculating the F content from the C content belonging to the FG, and assuming that the missing mass % belongs to oxygen. For H-PHI,

Element	H-PHI [mass %]	H-PHI [at. %]	PHI funct. [mass. %]	PHI funct. [at. %]
N	49.73	35.45	44.88	31.39
C	29.28	24.34	31.25	25.49
H	2.92	28.93	3.16	30.72
O*	18.07	11.28	17.85	10.93
F*	-	-	2.86	1.48
C/N ratio	0.5888	0.6867	0.6963	0.8120

only the assumption that oxygen is the missing mass was made. The elements with values that were obtained by calculation (O and F) are denoted with an asterisk.

XPS signal	Corresponding binding conditions	K-PHI [at. %]	PHI funct. [at. %]
F 1s (687.82 eV)	CF_3	0.42	4.54
O 1s (530.76 eV)	C=O	0.69	-
O 1s (531.34 eV)	C=O/O-H	-	2.67
O 1s (531.98 eV)	O-H	1.35	-
O 1s (532.97 eV)	C-O	-	0.26
C 1s (284.80 eV)	C-C/C-H	4.36	13.47
C 1s (287.41 eV)	C-OH	5.86	-
C 1s (288.23 eV)	N-C=N	27.86	31.01
C 1s (288.86 eV)	C=O	-	1.85
C 1s (292.93 eV)	CF_3	2.81	2.90
N 1s (398.54 eV)	C-N=C	32.42	26.66
N 1s (400.91 eV)	NH_x	6.97	11.23
N 1s (401.29 eV)	NH-(C=O)	-	1.41
N 1s (403.47 eV)	NO_x	1.17	1.03
N 1s (404.77 eV)	Pi-Pi*	1.31	1.43
K 2p3/2 (293.11 eV)	K^+	7.20	-
K 2p1/2 (295.91 eV)	K^+	7.00	-
K 2p (293.96 eV)	K^+	-	1.85
F 1s (total)	-	0.3	4.5
O 1s (total)	-	2.8	3.0
C 1s (total)	-	37.4	48.8
N 1s (total)	-	52.6	43.5
K 2s (total)	-	6.3	-

Table S5. Quantitative XPS measurements given in atomic %. The blue marked values are more relevant for functionalization to compare. The total values for each element are also given. For total K value, K 2s is used, as K 2p is overlapping with C 1s.

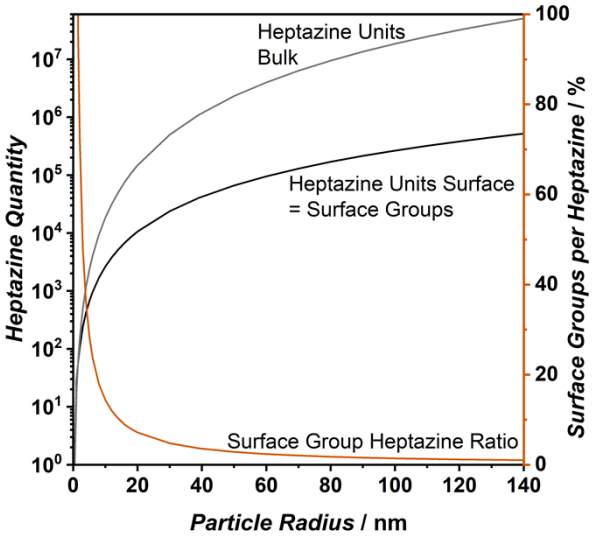

3.2. Figures

Figure S1. Relation between surface and bulk heptazine units, the surface group to heptazine ratio and the particle size of a spherical PHI particle. The number of heptazine units on the surface equals the number of available surface groups for functionalization in this calculation, as in an ideal structure, one heptazine on the surface would have one surface group.

Surface group calculation for figure S1:

All PHI related values for the calculation are taken from studies of H. Schlomberg *et al.*[9] For the calculation of the surface groups quantity, a spherical PHI particle consisting of round sheets was assumed. If the pore like PHI structure is completely intact without any defects on the edges, surface groups appear alternately every 1.34, 1.28 and 0.86 nm, giving an average of one surface group every 1.16 nm. Thus, for a round sheet, the number of surface groups (N_{SG}) can be calculated from the circumference (C) and the sheet radius (r(S)):

$$NSG(S) = {}^{C}/_{1.16\,nm} = {}^{2 \times \pi \times r(S)}/_{1.16\,nm}$$

The distance between the sheets (S) is 0.32 nm. The sheets are numbered in the following by starting with one sheet in the middle of the sphere (sheet S_0) and going to the sphere edge with decreasing sheet sizes, giving S_1, S_2, … until the last and smallest sheet of the sphere, giving S_n. Each sheet, except S_0, has a second, mirrored sheet with the same size. Thus, the total number of sheets in the sphere is n × 2+1. To calculate the number of surface groups for sheet S_0, the radius of the sphere is taken. Each further sheet is smaller, and the radius for those sheets can be calculated by drawing a triangle between the center of the sphere, the center of the sheet, and the sphere edge where the sheet lies. The two legs of the right-angled triangle are the radius of the sheet and the distance of the sheet from the middle of the sphere, given by the sheet distance c multiplied by the sheet number x. The hypotenuse is the radius of the spherical particle (r_p). The radius of each sheet (r(Sx)) can therefore be calculated as follows:

$$r(Sx) = \sqrt{r_p^2 - c^2 \times x^2}$$

Thus, the number of surface groups for any sheet is given by:

$$NSG(Sx) = {2 \times \pi \times \sqrt{r_p^2 - c^2 \times x^2}}/{1.16\ nm}$$

For the total number of surface groups (N_{SG}), it follows:

$$NSG = NSG(S0) + 2 \times NSG(S1) + 2 \times NSG(S2) + \ldots + 2 \times NSG(Sn)$$

With:

$$n = {r_p}/{c}$$

Therefore, the total number of surface groups of a spherical particle is calculated as follows:

$$NSG = {2 \times \pi}/{1.16\ nm} \times (r_p + 2 \times \sum_{x=1}^{n} \sqrt{r_p^2 - c^2 \times x^2}\ )$$

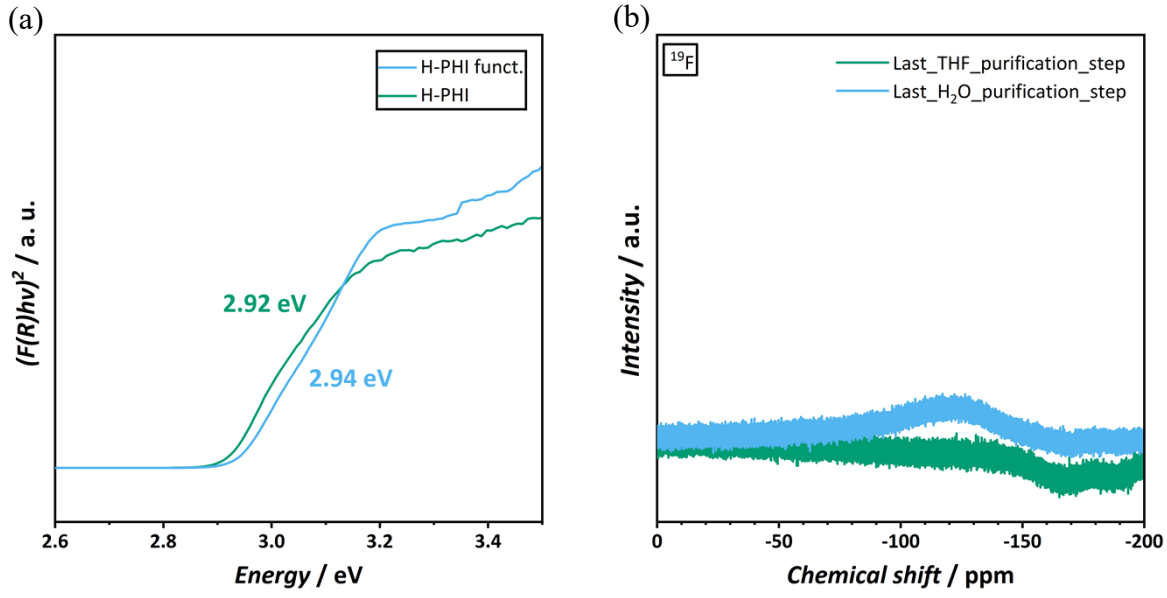

Figure S2. Tauc plot with calculated band gaps of optimized functionalized PHI compared to H-PHI (a) and Liquid ^{19}F NMR of the supernatants from purification which were used to ensure complete removal of unreacted material. Shown are the last washing steps with THF and water, respectively (b).

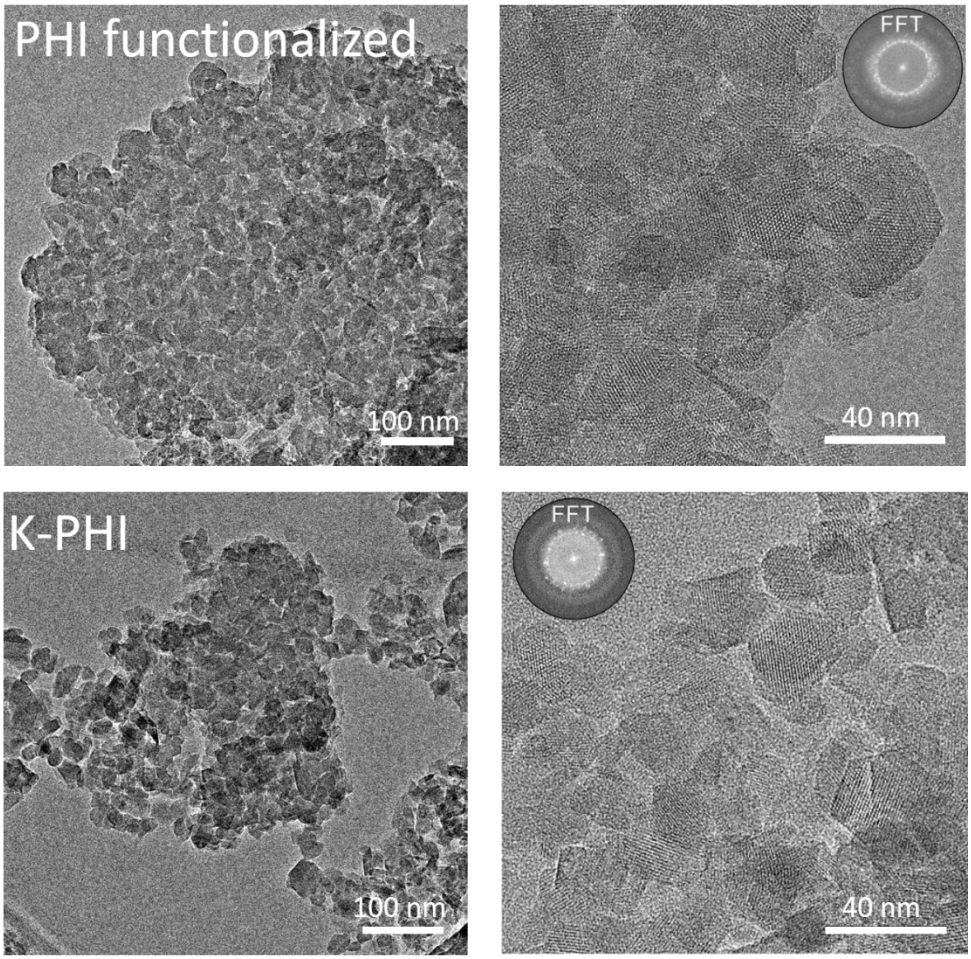

Figure S3. TEM images of the optimized functionalized PHI compared to K-PHI.

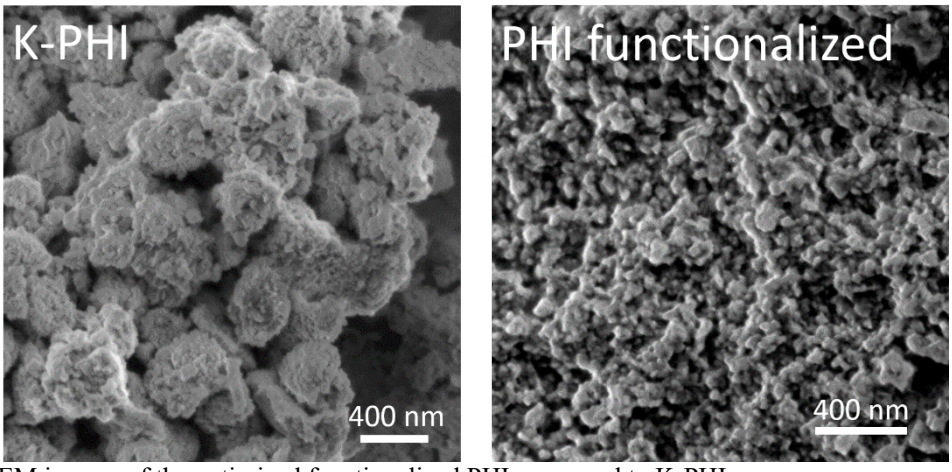

Figure S4. SEM images of the optimized functionalized PHI compared to K-PHI.

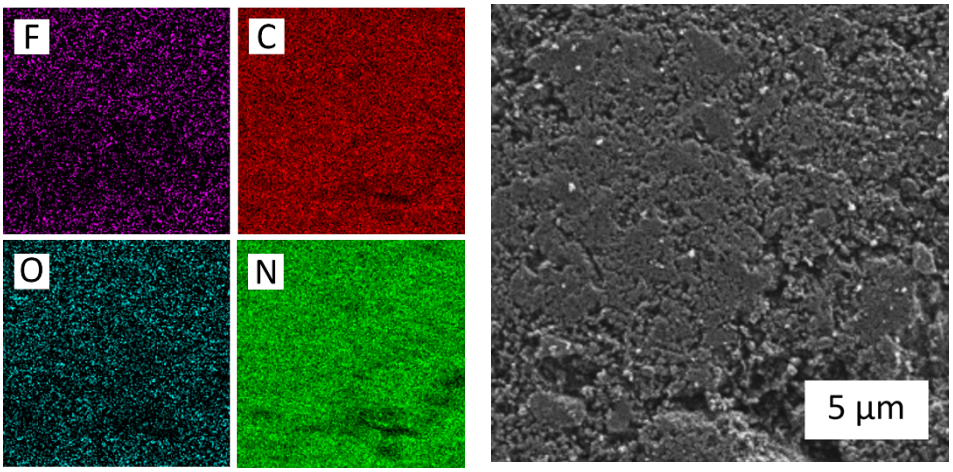

Figure S5. Elemental distribution measured by EDX for the optimized functionalized PHI. The SEM image of the depicted region is shown as well.

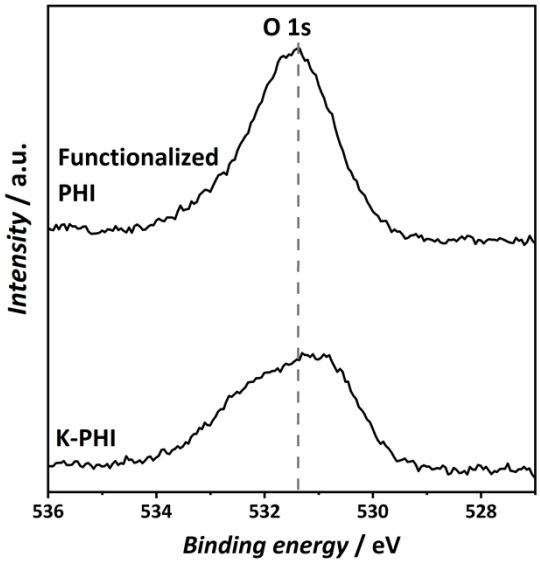

Figure S6. O 1s XPS spectrum of optimized functionalized PHI compared to K-PHI. The spectra are shown without peak fitting, as the O 1s signal is intrinsically rather broad and it has probably more than two species hidden in it.

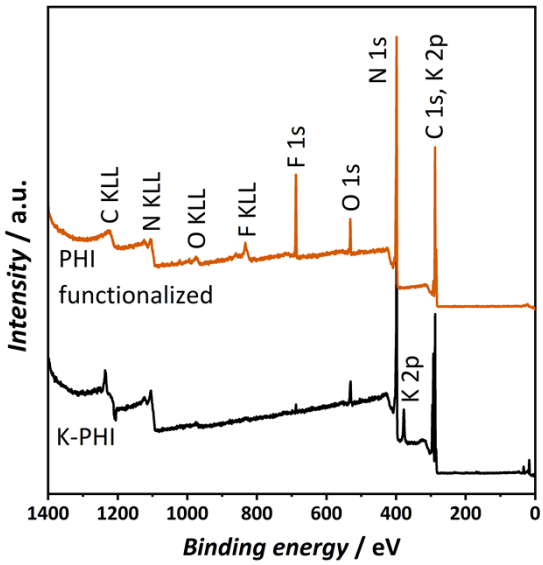

Figure S7. Total XPS spectrum of the optimized functionalized PHI compared to K-PHI.

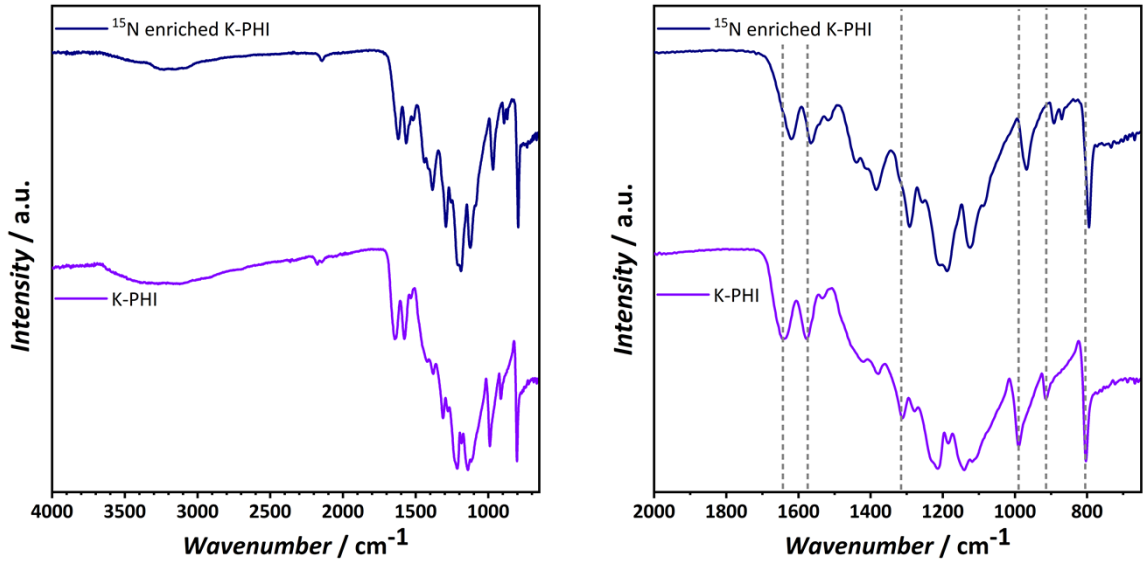

Figure S8. IR spectrum of ^{15}N enriched K-PHI compared to K-PHI. Visible are shifts in vibration bands due to ^{15}N enrichment. The total spectra are compared on the left, while zoomed versions with more relevant regions are depicted on the right.

3.3. Schemes

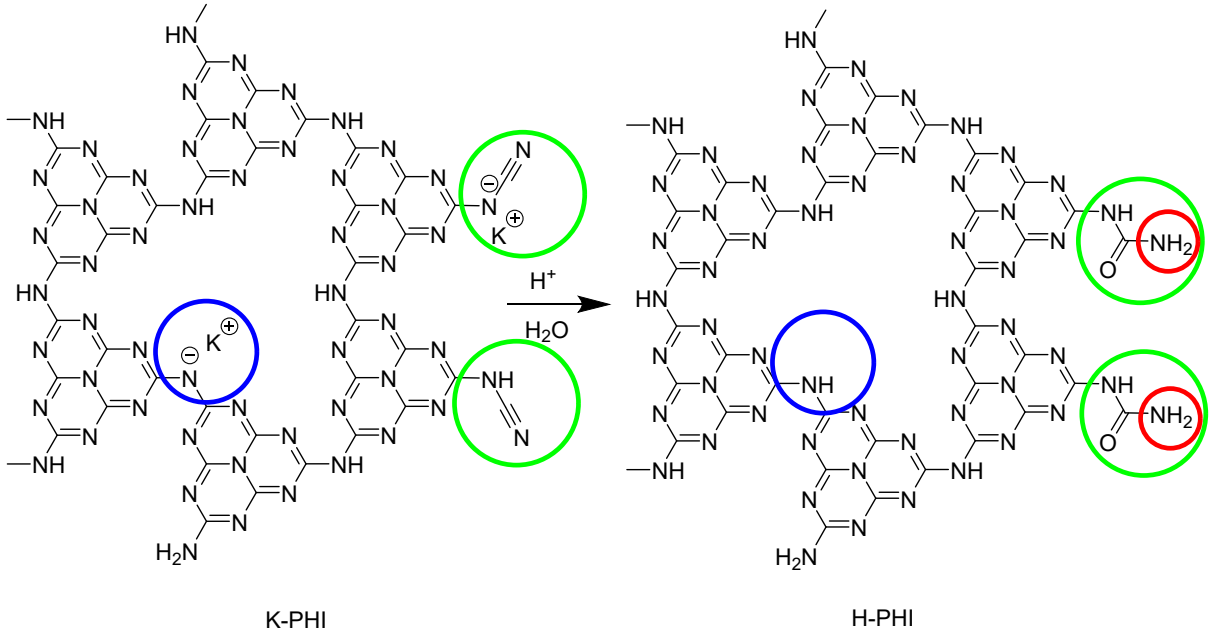

Scheme S1. Proposed structural changes occurring when K-PHI is treated under acidic conditions and H-PHI is formed. The main protonation takes place at the bridging, deprotonated amine groups (encircled in blue). The acidic catalyzed hydrolysis of the cyanamide groups is encircled in green, while the thereby formed amine groups are highlighted in red.

4. Further functionalization attempts

4.1. Overview

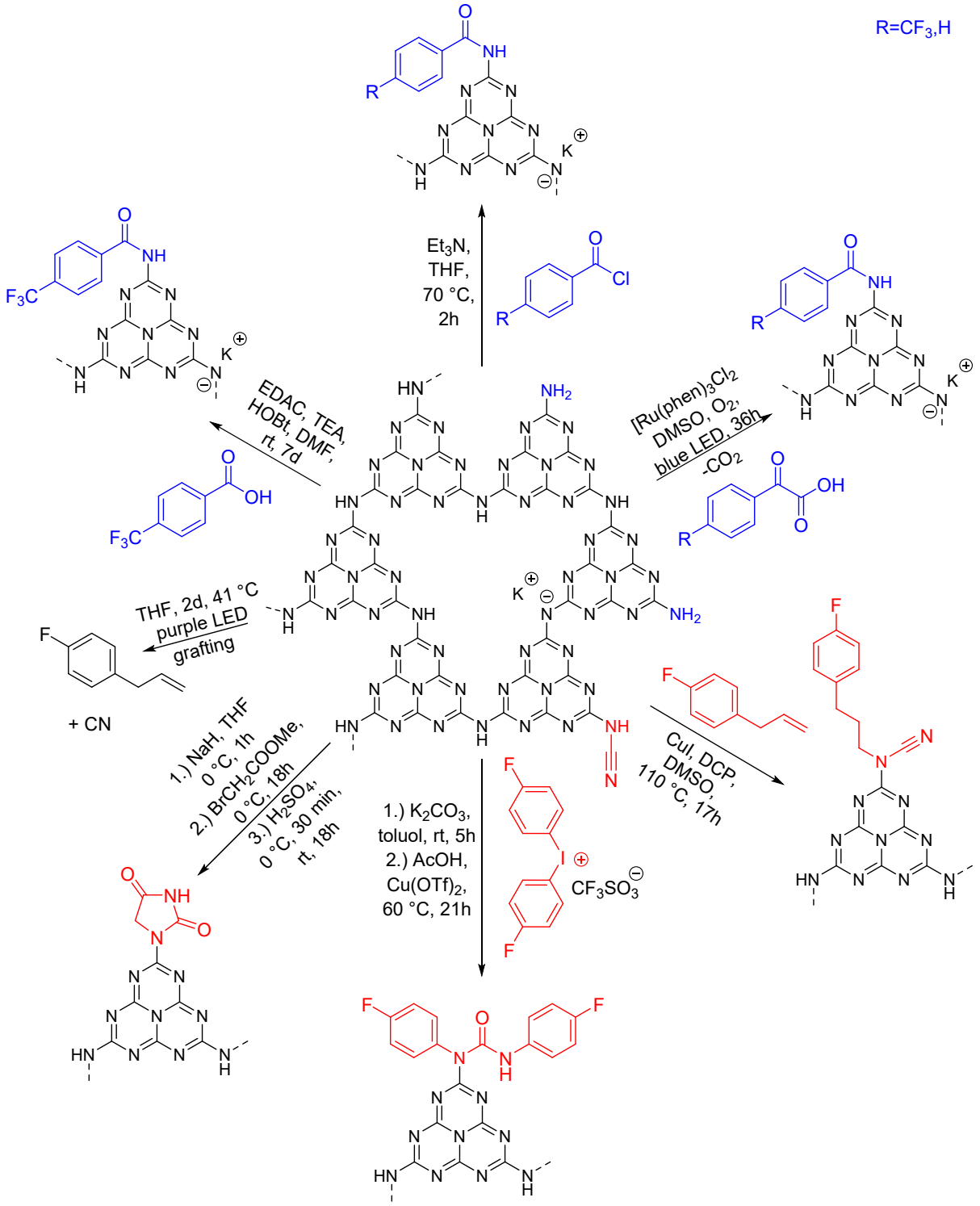

Scheme S2. Overview of functionalization attempts. Blue functionalizations targeting the amine group, red ones the cyanamide group.

4.2. Functionalization attempts on the NCN^- group of K-PHI

4.2.1. Cyanamide group functionalization of K-PHI with phenyl

Experimental procedure:

The cyanamide groups of K-PHI were functionalized with phenyl groups according to a method published by Li *et al.*[18] K-PHI (211 mg), bis-(4-fluorophenyl)-iodinium-trifluoromethane-sulfonate (233 mg, 0.50 mmol, TCI, ≥ 98 %) and K_2CO_3 (207 mg, 1.5 mmol, Merk, ≥ 99 %) were mixed with toluol (5.0 mL, Merk, ≥ 99.85 %). The suspension was stirred in a sealed microwave vessel under argon atmosphere for 5 h. Acetic acid (0.14 mL, 2.0 mmol, Merk, 100 %) was added dropwise to the mixture, before stirring for another 30 min. Bis-(4-fluorophenyl)-iodinium-trifluoromethanesulfonate (280 mg, 0.60 mmol) and copper(II) trifluoromethanesulfonate (361 mg, 0.10 mmol, TCI, ≥ 98 %) were added to the suspension. The mixture was stirred at 60 °C for 21 h. The product was centrifuged 13 times with tetrahydrofuran (16 k rpm, 15 min, 20 °C) and three times with DI water (22 k rpm, 10 min, 20 °C). A green solid was obtained after drying overnight at 60 °C.

Results:

Herein, we attempted to adapt a method reported by Li *et al.*[18] to functionalize the cyanamide groups of K-PHI with phenyl rings. The functionalization on the cyanamide groups of K-PHI was supposed to be detectable by a reduction of NCN^- vibrations in IR spectroscopy (Figure S9). A loss in signal is visible that is not completely explainable by the harsh reaction conditions, as the omission of starting material leads only to a small reduction of cyanamide. Additionally, the phenyl rings contain fluorine to investigate the completeness of washing with ^{19}F NMR (Figure S10) and measure ^{19}F ssNMR (Figure S11) afterwards to determine the yield. It has been discovered, that 13 times of washing was necessary to remove unreacted starting material. From ssNMR, a functionalization degree of 0.16 % (FG per heptazines) was calculated. Thus, the reaction was successful, and the low yield is explainable by the small amount of surface cyanamide groups compared to amine groups.

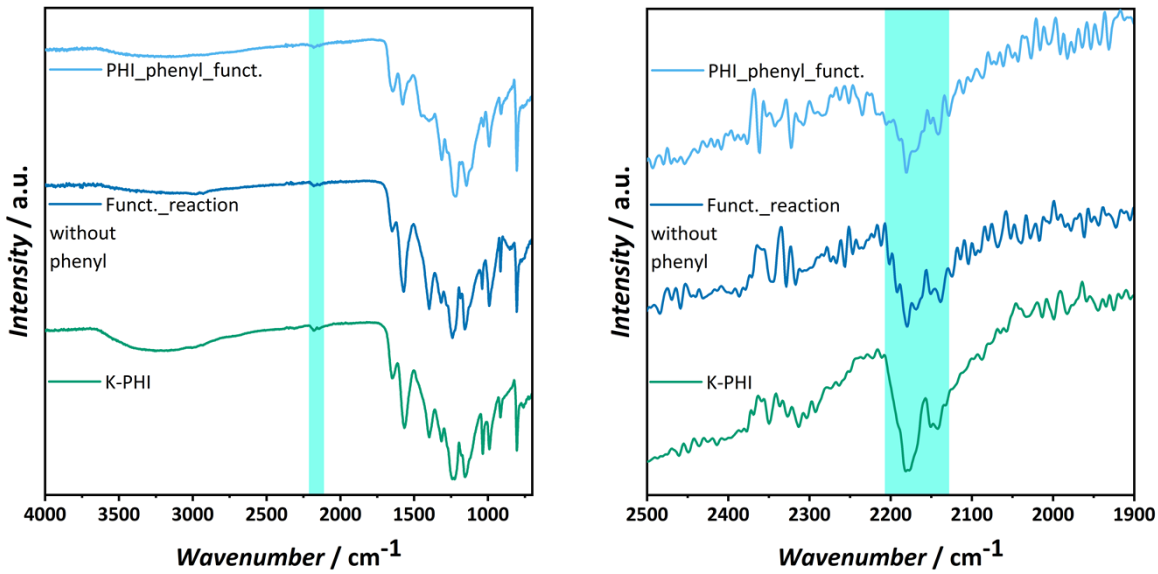

Figure S9. IR spectra of K-PHI compared to phenyl functionalized PHI and K-PHI under the functionalization reaction conditions without FG. The region of the NCN^- vibration is highlighted.

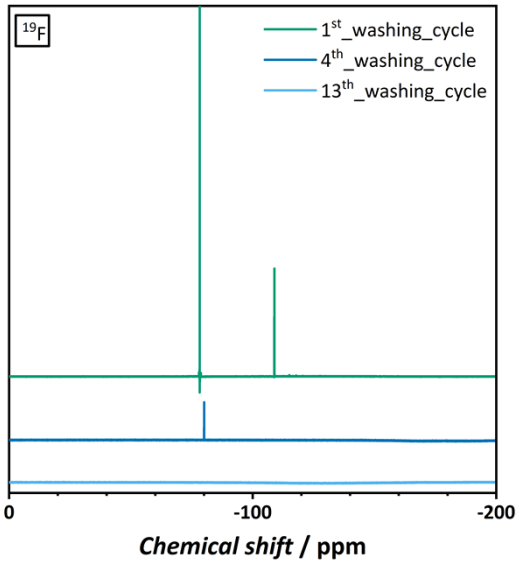

Figure S10. ^{19}F NMR to track the washing process of phenyl functionalized K-PHI.

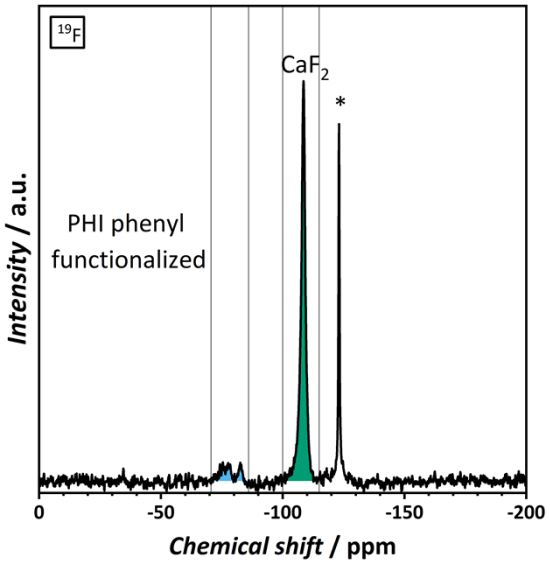

Figure S11. ^{19}F ssNMR of phenyl functionalized K-PHI for functional yield determination. The asterisk denotes a Teflon impurity.

4.2.2. Conversion of NCN^- groups into hydantoin rings

Experimental procedure:

The formation of a hydantoin ring at the cyanimide group of K-PHI was preformed based on the procedure published by Kumar *et al.*[19] Therefore, K-PHI (200 mg) was suspended in dry THF (10 mL) in a sealed microwave vessel. A 60% oil suspension of sodium hydride (60.0 mg, 2.5 mmol) along with dry THF (5.0 mL) was added in three portions at 0 °C. The reaction was carried out in argon atmosphere and stirred for 1 h under ice cooling. A solution of methyl bromoacetate (0.052 mL, 0.47 mmol, TCI, ≥ 98 %) and tetrahydrofuran (2.0 mL) was added at 0 °C and stirred for 18 h. The product was centrifuged two times with tetrahydrofuran and dichlormethane (16 k rpm, 15 min, 20 °C), respectively, followed by centrifugation with deionized water (22 k rpm, 10 min, 20 °C). The yellow solid was dried overnight at 70 °C. Afterwards, the dry yellow solid (200 mg, 0.47 mmol) and tetrahydrofuran (1.0 mL) were slowly added to a 0 °C cooled mixture of 50% H_2SO_4 (1.0 mL, Merk, ≥ 96 %). The reaction was stirred for 30 min at 0 °C and then 18 h at room temperature. The yellow product was washed until being pH neutral with deionized water followed by three times of centrifugation with deionized water (22 k rpm, 10 min, 20 °C) and dried overnight at 80 °C.

Results:

The attempt of functionalizing K-PHI with hydantion had several motivations. Hydantoin has chemical and biological importance, is harmless, can be synthesized from cyanamide groups[11] and is thus a great candidate to functionalize on the surface of K-PHI and detect the reduction of NCN^- groups due to functionalization. After the reaction, a lower cyanamide signal is visible in the IR spectrum (Figure S12). However, the signal is also reduced when no starting material responsible for ring closure is added. This is explainable by the formation of H-PHI during

synthesis, which also results in a reduced cyanamide signal. Nevertheless, the disappearance of cyanamide signal is reversible, if H-PHI is converted back to K-PHI. This can be observed when PHI treated under the functionalization's reaction conditions but without starting material is treated with KOH, as the cyanamide signal rises again. For the hydantoin functionalized sample, cyanamide vibrations are still not visible after KOH treatment, even though it was successfully converted back into K-PHI (Figure S13). This indicates a successful functionalization.

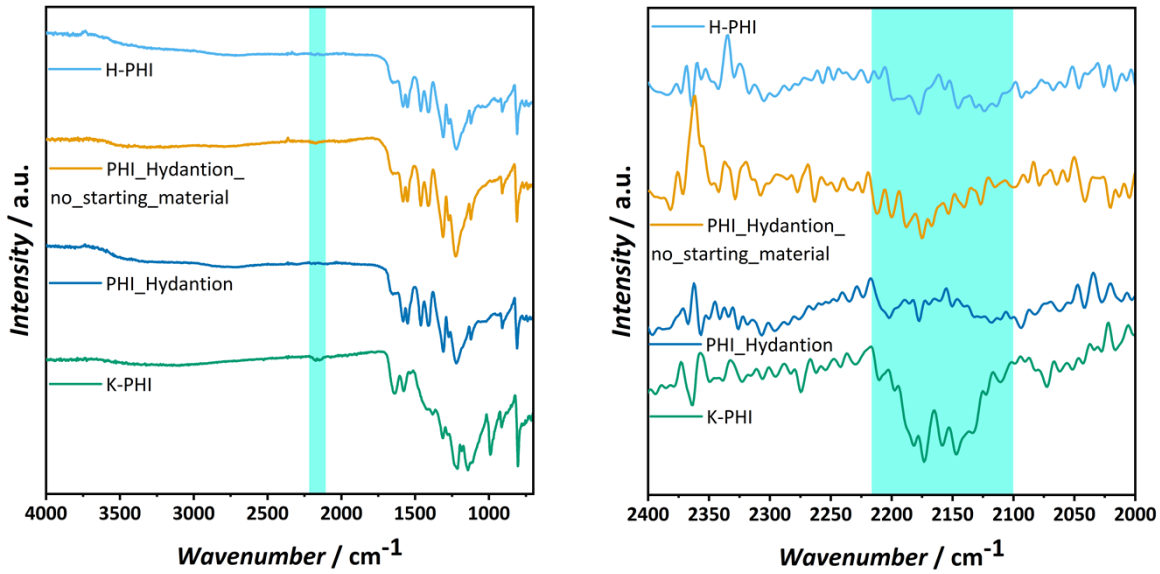

Figure S12. IR spectra of K-PHI and H-PHI compared to hydantoin functionalized PHI and PHI under the functionalization reaction conditions without starting material. The region of the NCN^- vibration is highlighted.

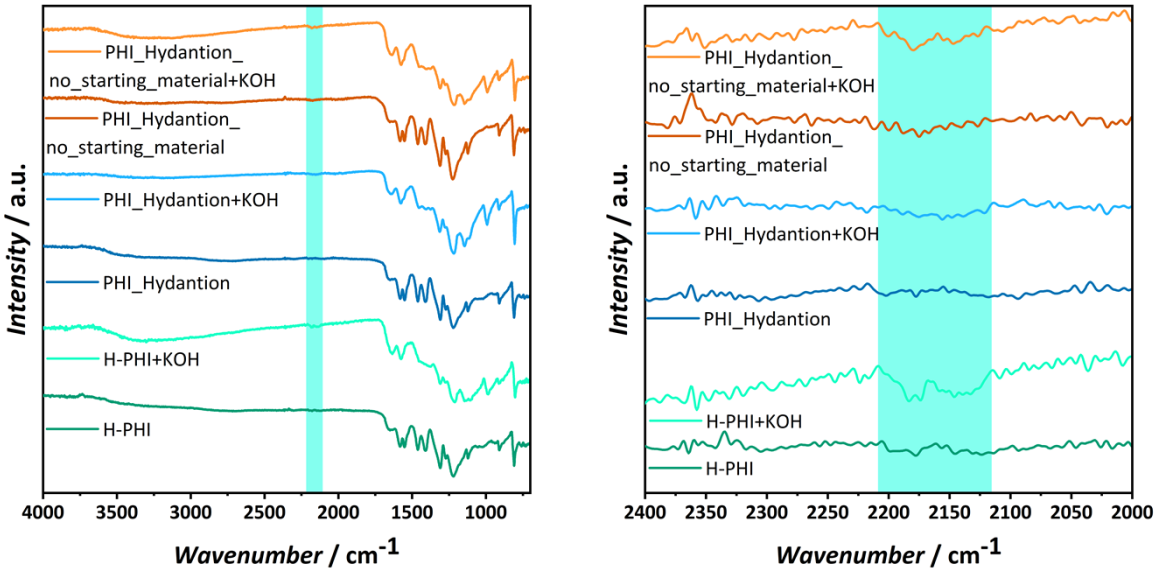

Figure S13. IR spectra of H-PHI, the hydantoin functionalized PHI and PHI under the functionalization reaction conditions without starting material along with their respective conversion to K-PHI with KOH treatment. The region of the NCN^- vibration is highlighted.

However, further analysis was inconclusive, as the functionalization always leads to similar results than the PHI under reaction conditions without the starting material for ring cyclization. Functionalized PHI has a zeta potential of -36.3 mV, a C/N ratio determined by EA of 0.73 (0.69 for untreated K-PHI and H-PHI) and the same band gap as H-PHI with 2.92 eV. The PHI under reaction conditions without starting material has a zeta potential of -34.3 eV and a C/N ratio of 0.76. When cobalt is tried to complex on the hydantoin unit and ICP-OES is measured after thoroughly washing both samples, 0.09 % for the unreacted and 0.19 % for the functionalized PHI is measured. However, the cobalt loading for K-PHI under the same cobalt ion treatment is 0.18 %, while for H-PHI it is 0.45 %. Thus, it is ambiguous if the functionalization was successful which shows the difficulty of analyzing surface functionalizations of K-PHI. Only the IR measurements after KOH treatment hints towards positive results.

4.2.3. Radical initiated alkylation

Experimental procedure:

The radical-initiated alkylation of K-PHI is based on a procedure published by Li *et al.*[20] For this functionalization, K-PHI (300 mg, 0.71 mmol), 1-allyl-4-fluorobenzene (0.096 mL, 0.71 mmol, Sigma-Aldrich, ≥ 97 %), CuI (13.5 mg, 0.071 mmol, Alfa Aesar, ≥ 98 %) and dicumylperoxide (576 mg, 2.1 mmol, Acros organics, ≥ 99 %) were added to dimethylsulfoxide (5.0 mL, Fisher chemicals, ≥ 99.9 %) in a sealed microwave vessel under argon atmosphere. The mixture was stirred for 17 h at 110 °C. Afterwards, the product was centrifuged three times with deionized water (22 k rpm, 10 min, 20 °C) and three times with dimethylsulfoxide

(16 k rpm, 15 min, 20 °C). The reaction product was dried overnight at 70 °C to yield a brown solid.

Results:

For radical initiated alkylation, a fluorine containing molecule was used to track the purification process and measure ^{19}F ssNMR afterwards. IR was also measured to detect changes in the target surface group, cyanamide, and UV-Vis was measured to determine optical changes. Both, IR (Figure S14) and UV-Vis (Figure S15) show the desired changes after functionalization. However, the absence of the cyanamide vibrations are also visible when no functionalization agent or heat is introduced, even though no H-PHI is formed. Furthermore, the UV-Vis spectrum is also changing in the visible region without functionalization agent, without heat or

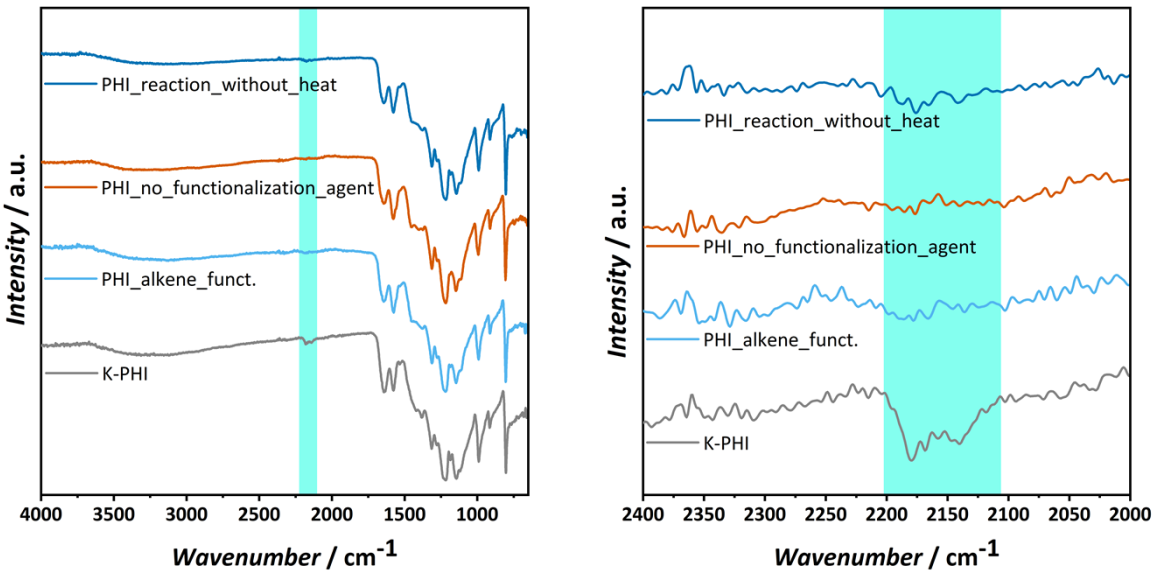

even when K-PHI is heated without any addition for the synthetic procedure.

Figure S14. IR spectrum of K-PHI compared to the radical functionalization attempt with alkene, the reaction without heat and the reaction without the alkene as functionalization agent.

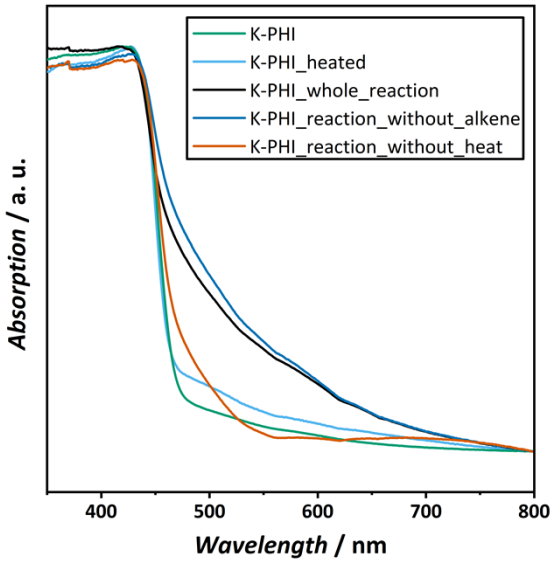

Figure S15. UV-Vis spectrum of K-PHI compared to the radical functionalization attempt with alkene, the reaction without heat, the reaction without the alkene as starting material and K-PHI that was heated to the reaction temperature in the reaction solvent but without additional reactants.

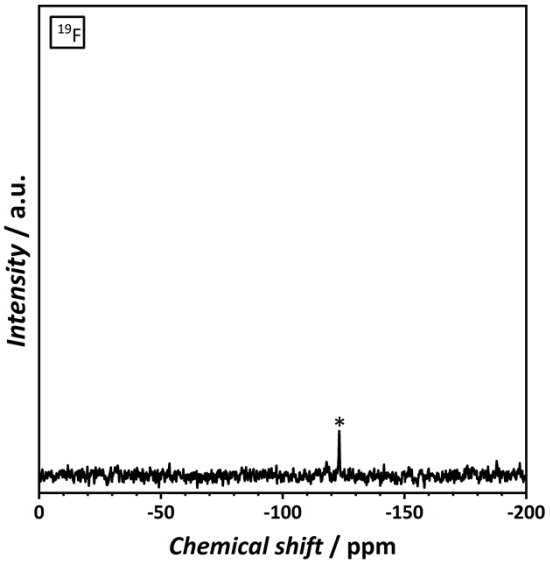

Figure S16. ssNMR of the radical functionalization with alkene showing only Teflon impurities.

From ssNMR measurements (Figure S16), it is visible that no FG is present in the solid and the only signal is a small Teflon contamination, proving that the functionalization was unsuccessful. This functionalization attempt therefore shows the difficulty of interpreting some analytic methods for the success of a surface functionalization. Any treatment to the system lead to the desired changes, but as visible in ssNMR, surface functionalization was never the reason for these transformations.

4.3. Functionalization attempts on the NH_2 groups of K-PHI

4.3.1. Radical initiated functionalization with α-keto acids

Experimental procedure:

For this synthesis, the starting material [(4-trifluoromethyl)phenyl]glyoxylic acid was synthesized as described in literature.[21] The functionalization was conducted based on an amide formation outlined by Liu *et al.*[21] K-PHI (200 mg) was mixed with the α-keto acid (phenylglyoxylic acid (Fisher chemicals, ≥ 97 %): 75 mg, 0.50 mmol or [(4-trifluoromethyl)phenyl]glyoxylic acid: 20 mg, 0.092 mmol) and dichlorotris(1,10-phenanthroline)ruthenium(II) chloride (4.1 mg, 0.0058 mmol or 3.7 mg, 0.0052 mmol, Sigma-Aldrich, ≥ 98 %) in DMSO (2.0 mL). After applying an O_2 atmosphere, the reaction mixture was stirred for 36 h under irradiation of blue LEDs (403 nm). Afterwards, the crude product was washed three times with DMSO and water (22k rpm, 10 min, 20 °C), respectively and dried at 70 °C overnight.

Results:

The next functionalization attempt had the amine group as target and harsh conditions with a radical initiated reaction have been chosen to ensure a reaction. IR was measured to check for changes caused by the functionalization, like an increased C=O vibration or similar signals (Figure S17). However, as described before, IR lead to ambiguous results, as all parameter changes resulted in similar differences compared to K-PHI. Thus, K-PHI was mixed with benzoic acid without a reaction in different ratios to investigate how different functionalization yields might influence the IR spectrum (Figure S18). As visible, nearly no vibrations are changing, even with a theoretical functionalization degree of 20 % (FG per heptazine). Only a slowly increasing band at about 730 cm^{-1} shows the presence of benzoic acid, but this peak is not visible in the actual functionalization with PGA.

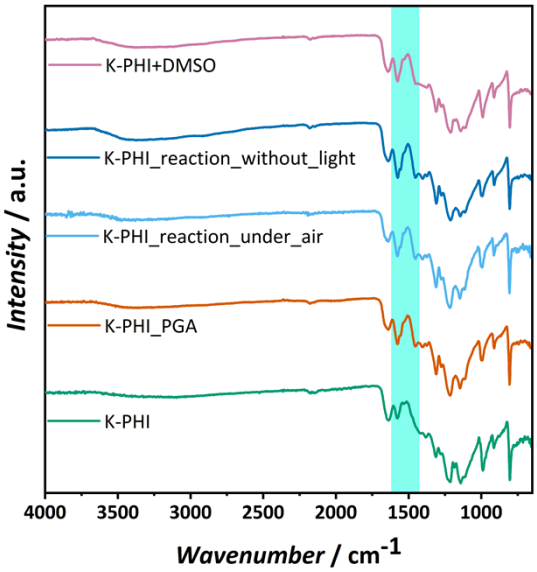

Figure S17. IR spectrum of K-PHI compared to the radical functionalization attempt with phenyl glyoxylic acid (PGA), the reaction without light, the reaction under normal air instead of an oxygen atmosphere and K-PHI only treated with DMSO.

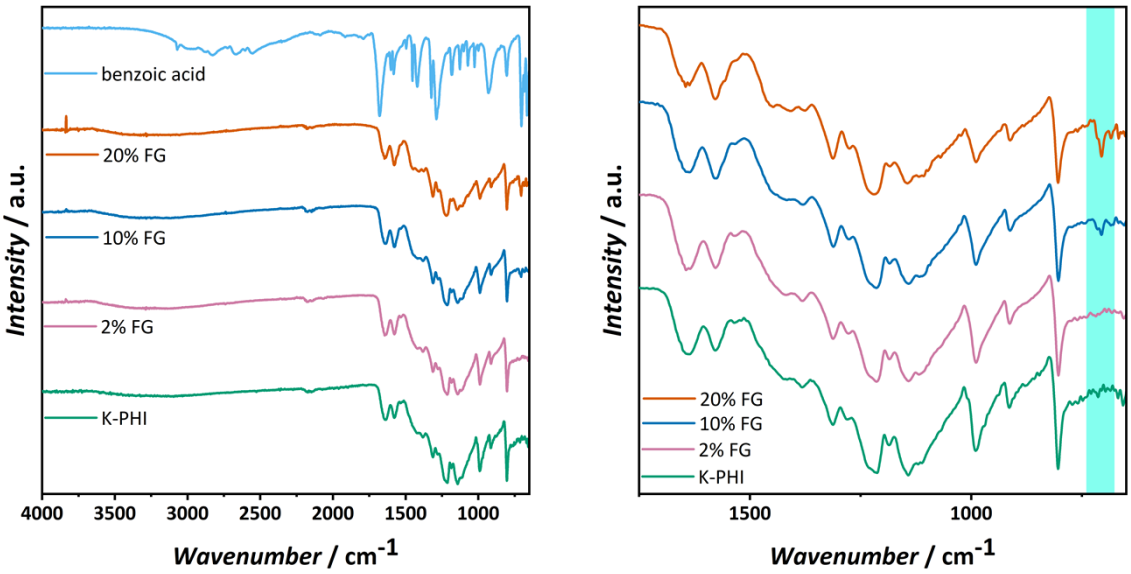

Figure S18. IR spectrum of K-PHI mixed with different amounts of benzoic acid to exemplify the difficulty of IR to detect functionalization. Theoretical yields between 2 % and 20 % are shown.

To overcome the detection problem from IR and other analytics for functionalization, PGA with a CF_3 group in para position of the phenyl ring was chosen to enable ^{19}F NMR measurements. After complete purification verified by liquid ^{19}F NMR, ^{19}F ssNMR was measured to determine the success and yield of the functionalization (Figure S19). With this method, a yield of 0.13 % was calculated.

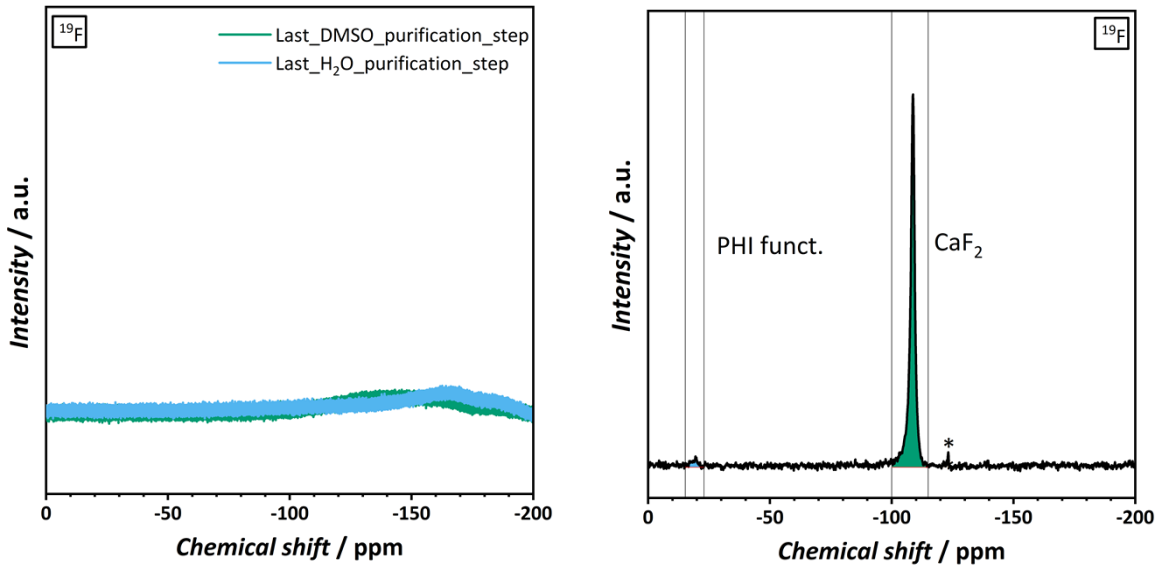

Figure S19. Liquid ^{19}F NMR of the last washing step with DMSO and water and ^{19}F ssNMR for quantifying the functionalization yield. The asterisk denotes a Teflon impurity.

4.3.2. Amide formation on K-PHI derived from a melon based functionalization

Experimental procedure:

K-PHI was tried to functionalize according to a procedure by Ma *et al.*[22] 1-Ethyl-3-(3-(dimethylaminopropyl)carbodiimide, HCl (EDAC, 7.6 mg, 0.049 mmol, Carl Roth, ≥ 99 %) and triethylamine (5.5 µL, 0.040 mmol were added to a suspension of 4-(trifluormethyl)benzoic acid (3.8 mg, 0.020 mmol, TCI, ≥ 98 %) in DMF (13 mL, VWR chemicals, ≥ 99.9 %). After stirring for 20 min at room temperature, 1-hydroxybenzotriazole (5.4 mg, 0.040 mmol, Sigma-Aldrich, ≥ 97 %) in DMF (1.3 mL) was added and the mixture was stirred for 1 h. In the meantime, a suspension of K-PHI (200 mg) in DMF (4.0 mL) was prepared by sonicating for 40 min. The suspension was transferred to the reaction mixture by using 1.0 mL DMF additionally and the reaction was kept stirring for 7 d at room temperature. The crude product was washed three times with DMF and water (22k rpm, 10 min, 16 °C), respectively and dried at 60 °C overnight.

Results:

Many functionalization attempts for melon based carbon nitride have already been published. Therefore, one of the most reasonable procedures, where the removal of starting material was also tracked,[22] was tested on K-PHI to investigate if the synthesis is feasible as well. However,

only the structural motif from the FG group was used to see if and how good the functionalization works in general. Thus, instead of Co-quaterpyridine with a carboxylic acid group, 4-(trifluormethyl)benzoic acid was used as FG. A fluorine containing compound was chosen to track the purification and determine the yield *via* ssNMR afterwards (Figure 20). A yield of 0.07 % was reached, which is slightly higher but in accordance with the yield of 0.03 % for melon based carbon nitride from the original publication.

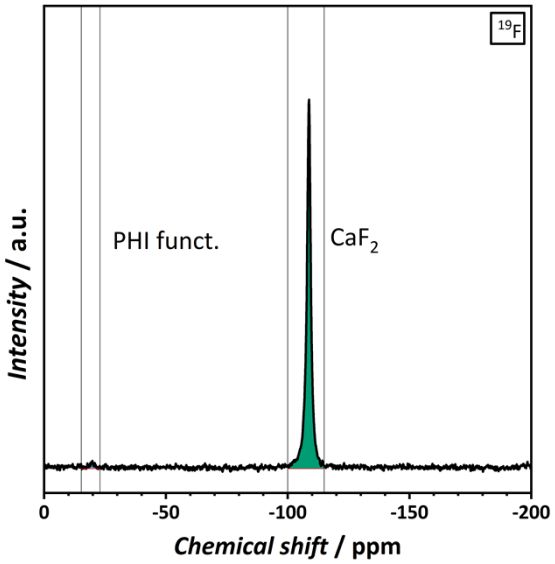

Figure S20. ^{19}F ssNMR for quantifying the functionalization yield.

4.4. Reproduction of grafting alkenes on carbon nitrides

Experimental procedure:

The grafting on carbon nitride method was conducted according to the description of Cao *et al.*[23] A suspension of carbon nitride (melon or K-PHI, 100 mg) in THF (15 mL) was sonicated for 30 min. 1-Allyl-4-fluorobenzene (100 µL, 0.74 mmol) was added and the mixture was set under an argon atmosphere by flushing argon for 2 h. The reaction was stirred for 2 d under irradiation with purple LEDs, which resulted in a constant temperature raise to 41 °C. Next, the crude product was washed three times with THF (16k rpm, 15 min, 20 °C) and dried at 50 °C overnight.

Results:

Recently, a procedure for grafting FG on the surface of melon based carbon nitride *via* radical reaction was published.[23] However, as it is usually difficult distinguish pore intercalated from covalently or not covalently bonded FGs, the binding situation in this work is also unclear, but it is rather assumed that the bond is non-covalent. As in our work, a good indicator was presented to estimate if a covalent bond has formed, we also applied our strategy to the published synthesis. Similar to the last section, only the structural motif responsible for the

reaction was used, which is an alkene rest. We again took a fluorine containing FG to detect the purification process to remove non-covalent bonded material (Figure S21). Afterwards, ssNMR was measured to investigate if covalently bonded FGs are left. The functionalizations were tried for melon (Figure S22) and K-PHI (Figure S23). As visible, no FG is left after washing, showing that the grafting on method is a non-covalent process.

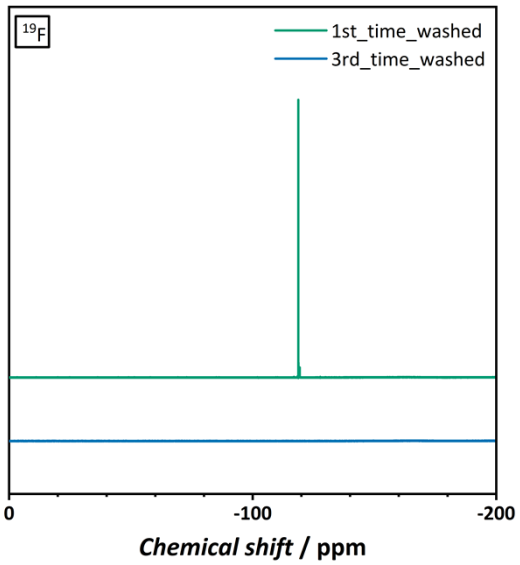

Figure S21. Exemplary ^{19}F NMR to track the washing process of grafting a FG on the surface of K-PHI.

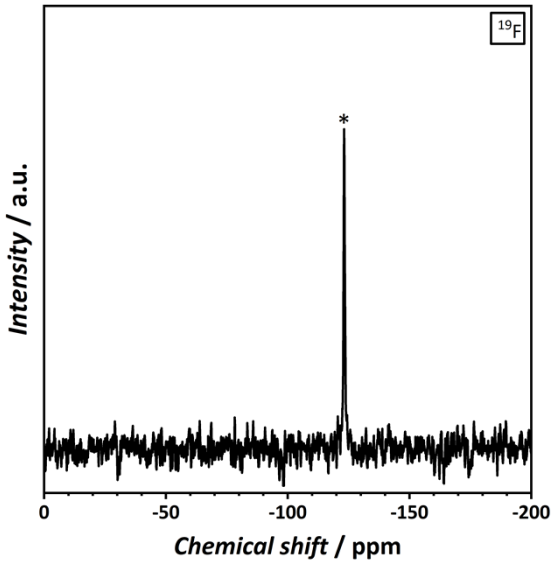

Figure S22. ^{19}F ssNMR of melon after washing only showing a Teflon impurity, indicated by an asterisk.

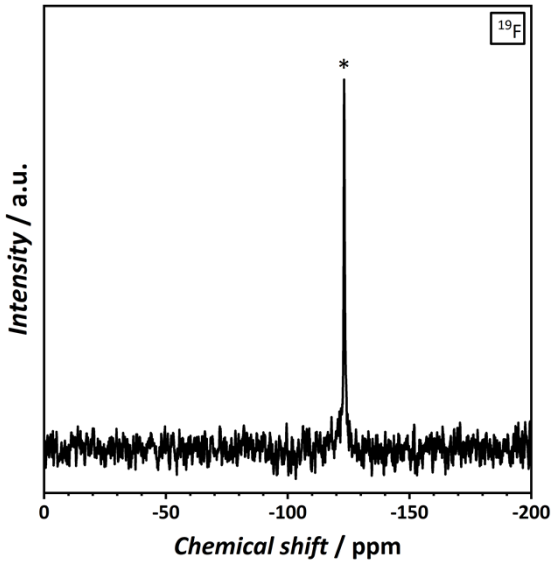

Figure S23. ^{19}F ssNMR of K-PHI after washing only showing a Teflon impurity, indicated by an asterisk.

5. Analytic guideline for carbon nitride functionalization

Despite demonstrating the feasibility of carbon nitride functionalization, analysis remains challenging, particularly when fluorine incorporation is impractical for intended applications. Therefore, we want to provide guidelines for the characterization of carbon nitride functionalizations. The most important step before analysis is to ensure complete removal of unreacted FGs. In this work, ^{19}F NMR measurements of the supernatant were mainly used to check the purification progress. For non-fluorine containing FGs, we recommend to check the supernatant by ^{1}H NMR, as it is a sensitive nucleus and shows unreacted organic materials. Additionally, it must be ensured that changes detected by any analytic method are not resulting from the reaction conditions itself. Especially for catalytic experiments, comparing experiments with carbon nitrides treated under the synthetic conditions for functionalization but without the FG are necessary.

Up to now, functionalization attempts for carbon nitrides have been mainly characterized by inductively coupled plasma mass spectrometry (ICP-MS)[28] or optical emission spectroscopy (ICP-OES),[11,22] elemental analysis (EA),[11] thermogravimetric analysis (TGA),[11,24] infrared (IR)[22,28] and Raman spectroscopy, X-ray photoelectron spectroscopy (XPS),[11,22,24,28] Zeta potential,[11] Ultraviolet–Visible (UV-Vis)[11,22,24] spectroscopy and nuclear magnetic resonance (NMR) spectroscopy.[11] However, all these analytic methods have some limitations, especially for carbon nitride surface analysis and quantification.

ICP-OES and ICP-MS is suitable for the quantification of the overall amount of several elements in a sample with high sensitivity and are thus good methods to calculate the surface functionalization in comparison to the bulk particles. However, carbon, nitrogen and hydrogen are too light to be quantified, so the inserted functional group must contain heavier elements to be detectable. When coordinative bonded metals are part of the functional group, it is hard to determine if all metals are bonded to the functional group after the synthesis. Metals might also coordinate to the amine groups of PHI or be washed out during the cleaning process, so the metal content cannot be directly correlated to the yield of functionalization. In addition, the detection limit depends on multiple parameters like the instrument, experimental conditions, the element itself and interferences with other elements.[29]

Elemental analysis is inexpensive and can also be used to quantify the total amount of functional groups per bulk material. It is mainly used to quantify the carbon, nitrogen, hydrogen and sulfur content. The first problem for carbon nitride is that EA works best if only the functional group contains these elements, and not the nanomaterial itself. Thus, carbon nitrides are not the most suitable nanomaterials for functionalization analysis by EA. The second problem is a low sensitivity.[29] The permissible deviation is about 0.3 %. Therefore, a calculated yield of 0.46 mol % can result only from deviations, if an exemplary organic material as functional group with eight carbon atoms per molecule, like the one we used in our studies, is assumed. Larger organic functional groups are easier to detect, but one should be certain that unreacted material is removed and that variations of the elemental composition do not result from structural changes from the bulk material or solvent intercalations. Thus, we recommend EA as

quantitative method only if the yield of functionalized heptazines exceeds 1 mol % or the functional group contains respectively more carbon.

TGA is fast, simple to prepare, and a good method for analyzing the surface of many, especially inorganic surfaces. However, a variety of contaminations and other effects can also lead to a mass loss during the heating process.[29] An example is remaining solvent, which is primarily a problem for K-PHI having pore intercalated water that already shows a significant loss of mass and can vary between samples.[9] Hence, the origin of the measured mass loss can be ambiguous, making quantification hard. However, the coupling of TGA mass loss with a mass spectrometer or other analytical devices helps to analyze the evaporated molecules and can provide insights about the surface of carbon nitrides, if other signal sources are excluded.

Vibrational spectroscopy like IR is a good method to give fast information about chemical bonds. For carbon nitrides, IR spectroscopy is helpful to differentiate structures. Vibrational spectroscopy is widely used for qualitative analyses, but less for quantitative investigations. Nevertheless, quantitative analysis is also possible, but intricate.[29] However, in regard to carbon nitrides and their surface functionalization's with an expectable low yield, quantitative as well as qualitative functional group (FG) analysis is almost impossible. The main problem are the strong vibrations in regions, where most functional groups have their characteristic bands as well. This is exemplified in Figure S18. K-PHI was mixed physically with different amounts of benzoic acid, a possible candidate for reactions with surface amine groups. Nearly no changes are visible between 800 and 1800 cm^{-1}. Only at about 700 cm^{-1}, a clear change is detectable, but with a high FG content of 10 mol % of functionalized heptazines. For lower yields like 2 mol % and for screening experiments, IR is rather not suitable. Another problem is that some reaction conditions also result in different vibration bands, even without the desired functional group. Thus, band assignment is not always straightforward. Especially for K-PHI, IR vibrations can easily change due to protonation. An example is shown in Figure S12. The aim for this functionalization attempt was to convert the NCN^- group in a hydantion ring. The NCN^- signal of K-PHI is highly visible at about 2200 cm^{-1}, so a change due to functionalization should be easy to detect. However, as visible, the loss of the NCN^- signal and the additional structural changes could also be explained by the formation of H-PHI, leaving with an ambiguous interpretation towards the success of the functionalization. Thus, the main usage for IR was found to ensure the structure was not destroyed by the functionalization procedure.

XPS is a standard method for surface analysis. The sample is irradiated with an X-ray beam and information on the elements present on the surface along with information about their binding situation can be obtained. Drawbacks are a low penetration depth of usually only 10 nm and a more difficult preparation than methods described before. For preparation, a very clean procedure is important to prevent contamination of the surface. While quantification of FGs on the surface is difficult but possible,[29] it is impossible to determine the ratio of FG to bulk material due to the low penetration depth. Also for carbon nitrides, FGs with other elements than carbon, nitrogen and hydrogen are useful again to better differ FG signals from the carbon nitride surface. If all these difficulties were overcome, XPS is one of the best methods to gain information about the surface of a material.

Electrochemical measurements of the surface to detect changes in particle charge, solubility, or the pH value are useful to observe structural changes.[29] For carbon nitrides, mainly the Zeta potential is measured to determine the particle charge and thereby, the suspension stability. Even though it is expedient for detecting surface changes, especially when the polarity or charge of the FG differs a lot from the carbon nitride surface, it is important to ensure the zeta potential change actually results from the FG. The problem can be exemplified by the attempt to convert the NCN^- group in a hydantion ring that was also mentioned in the IR description. The used K-PHI has a Zeta potential of - 50 (±2) mV at pH=7. The protonated version of PHI has a reduced potential of - 48 (±3) mV. After 18 h of the functionalization reaction, the Zeta potential has changed to - 36 (±2) mV. However, if no starting material is inserted into the reaction to form the hydantoin ring, the Zeta potential also changes significantly to - 34 (±2) mV. Thus, it is not possible to conclude a successful functionalization from Zeta potential measurements, as the structure of PHI also changes due to the reaction conditions. This problem has to be excluded when Zeta-potential is used as an analytic method for post synthetic surface modifications.

UV-Vis spectroscopy is often used to characterize functionalizations, especially with dye molecules. In a recent investigation of Co-qpy functionalized carbon nitride, UV-Vis was also suggested to serve as method to detect the removal of FG during the purification process.[22] However, structural changes and other effects can influence the UV-Vis spectrum of carbon nitrides as well. This is exemplified in Figure S15 for an unsuccessful functionalization attempt on cyanamide groups via a radical reaction using an alkene (see section 4.2.3.). The reaction mixture was heated to 110 °C. Different reaction parameters were left out to investigate the influence on the absorption. As visible, every parameter change results in a different UV-Vis spectrum. Under normal reaction conditions and without the alkene starting material, a flatter absorption decrease at wavelengths above 450 nm is visible. A similar but less distinct development proceeds if K-PHI is heated. When the reaction is conducted without heating, a combination of a flat decrease and an additional small absorption between 600 and 800 nm can be seen. In literature, a similar flat decrease is visible, when the starting material is only added and removed again from the system.[30] In another example, it is shown, that an unreacted dye starting material has an almost similar effect on the spectrum as bonded material. Nevertheless, it was discovered that a difference of 10 nm between the absorption maxima of reacted and unreacted material helped for allocation.[31] In conclusion, if the as described reasons for a change in the absorption are excluded, UV-Vis can serve as a method to detect functionalization. However, due to the huge possibility of other effects resulting in changes for a carbon nitride spectrum, it should rather be used as an auxiliary analytic method.

NMR spectroscopy is another method to detect structural changes. The advantage of NMR spectroscopy compared to many other analytic methods is, that not only the presence of different atoms can be shown, but difference in the binding situations can also be investigated and quantified. Especially in liquid NMR spectroscopy, the change between surface bonded and not bonded FG is visible.[29] Carbon nitrides usually form huge agglomerates that are insoluble, so only ssNMR is usable as analytic method. The broad and the large signals of

carbon nitrides for carbon, nitrogen and hydrogen complicate the surface analysis with ssNMR for organic functional groups. However, if isotopic enriched FGs are used or other nuclei like fluorine or phosphorous are constituents of the FG, it is possible to gain qualitative and quantitative information on the success of the functionalization.

Ultimately, every analytic method has its strengths and limitations for carbon nitride surface investigation. By combining multiple methods, it is possible to proof the success of the functionalization from the resulting indications. However, the exclusion of detecting unreacted, non-covalently bonded FGs or only slight structural changes on the carbon nitride bulk structure is essential. If possible, the insertion of a marker element that is not part of the carbon nitride structure is advisable to simplify the characterization. This supports analytic methods to unambiguously differ between the carbon nitride structure and the FG. Especially for the expected low yield and for the first screening experiments to evaluate if the reaction conditions chosen even work, this principle is very helpful.

6. References

1 R. K. Harris, E. D. Becker, S. M. Cabral De Menezes, R. Goodfellow, and P. Granger, *Pure Appl. Chem.*, 2001, **73**, 1795–1818.

2 K. J. D. Mac Kenzie and M. E. Smith, *Pergamon*, 2002, **6**.

3 B. Metz, X. L. Wu and S. O. Smith, *Journ. Magn. Reson. Ser. A*, 1994, **110**, 219.

4 B. M. Fung, A. K. Khitri and K. Ermolaev, *J. Magn. Res.*, 2000, **142**, 97.

5 J. Schaefer, T.A. Skokut, E.O. Stejskal R.A. McKay, and J. E. Varner, *Proc. Nat. Acad. Sci.*, 1981, **78**, 5978.

6 J. Schaefer, E.O. Stejskal, J.R. Garbow, and R.A. McKay, *J. Magn. Reson.*, 1984, **59**, 150–156.

7 M. C. Biesinger, *Appl. Surf. Sci. Adv.*, 2022, **597**, 153681.

8 N. Fairley, V. Fernandez, M. Richard-Plouet, C. Guillot-Deudon, J. Walton, E. Smith, D. Flahaut, M. Greiner, M. Biesinger, S. Tougaard, D. Morgan and J. Baltrusaitis, *Appl. Surf. Sci. Adv.*, 2021, **5**, 100112.

9 H. Schlomberg, J. Kroger, G. Savasci, M. W. Terban, S. Bette, I. Moudrakovski, V. Duppel, F. Podjaski, R. Siegel, J. Senker, R. E. Dinnebier, C. Ochsenfeld and B. V. Lotsch, *Chem. Mater.*, 2019, **31**, 7478–7486.

10 J. Kröger, A. Jiménez-Solano, G. Savasci, V. W. h. Lau, V. Duppel, I. Moudrakovski, K. Küster, T. Scholz, A. Gouder, M. L. Schreiber, F. Podjaski, C. Ochsenfeld and B. V. Lotsch, *Adv. Funct. Mat.*, 2021, **31**, 2102468.

11 J. Kröger, A. Jiménez-Solano, G. Savasci, P. Rovó, I. Moudrakovski, K. Küster, H. Schlomberg, H. A. Vignolo-González, V. Duppel, L. Grunenberg, C. B. Dayan, M. Sitti, F. Podjaski, C. Ochsenfeld and B. V. Lotsch, *Adv. Energy Mater.*, 2020, **11**, 2003016.

12 E. Wirnhier, M. Doblinger, D. Gunzelmann, J. Senker, B. V. Lotsch and W. Schnick, *Chem. Eur. J.*, 2011, **17**, 3213–3221.

13 H. May, *J. appl. Chem.* 1959, **9**, 340–344.

14 V. W. Lau, M. B. Mesch, V. Duppel, V. Blum, J. Senker and B. V. Lotsch, *J. Am. Chem. Soc.*, 2015, **137**, 1064–1072.

15 L. Zhang, X.-j. Wang, J. Wang, N. Grinberg, D. Krishnamurthy and C. H. Senanayake, *Tetrahedron Lett.*, 2009, **50**, 2964–2966.

16 S. Shibata, Y. Masui and M. Onaka, *Bull. Chem. Soc. Jpn.* 2020, **93**, 663–670.

17 J. A. Kepler, J. W. Lytle and G. F. Taylor, *J. Label. Compd. Radiopharm.* 1974, **10**, 683–987.

18 P. Li, G. Cheng, H. Zhang, X. Xu, J. Gao and X. Cui, *J. Org. Chem.*, 2014, **79**, 8156–8162.

19 V. Kumar, M. P. Kaushik and A. Mazumdar, *Eur. J. Org. Chem.* 2008, **2008**, 1910–1916.

20 Z. Li, Y. Xiao and Z.-Q. Liu, *Chem. Commun.* 2015, **51**, 9969–9971.

21 J. Liu, Q. Liu, H. Yi, C. Qin, R. Bai, X. Qi, Y. Lan and A. Lei, *Angew. Chem. Int. Ed. Engl.*, 2014, **53**, 502–506.

22 B. Ma, G. Chen, C. Fave, L. Chen, R. Kuriki, K. Maeda, O. Ishitani, T. C. Lau, J. Bonin and M. Robert, *J. Am. Chem. Soc.*, 2020, **142**, 6188–6195.

23 Q. Cao, B. Kumru, M. Antonietti and B. Schmidt, *Macromolecules*, 2019, **52**, 4989–4996.
24 W. Lu, T. Xu, Y. Wang, H. Hu, N. Li, X. Jiang and W. Chen, *Appl. Catal. B: Environ.*, 2016, **180**, 20–28.
25 G. Dong, L. Yang, F. Wang, L. Zang and C. Wang, *ACS Catalysis*, 2016, **6**, 6511–6519.
26 K. A. Lin and J. T. Lin, *Chemosphere*, 2017, **182**, 54–64.
27 C. D. Windle, A. Wieczorek, L. Xiong, M. Sachs, C. Bozal-Ginesta, H. Cha, J. K. Cockcroft, J. Durrant and J. Tang, *Chem. Sci.*, 2020, **11**, 8425–8432.
28 Y. Wei, L. Chen, H. Chen, L. Cai, G. Tan, Y. Qiu, Q. Xiang, G. Chen, T. C. Lau and M. Robert, *Angew. Chem. Int. Ed. Engl.*, 2022, **61**, e202116832.
29 D. Geissler, N. Nirmalananthan-Budau, L. Scholtz, I. Tavernaro and U. Resch-Genger, *Mikrochim. Acta*, 2021, **188**, 321.
30 C. Zhang, J. Liu, X. Liu and S. Xu, *Catal. Sci. Technol*., 2020, **10**, 1609–1618.
31 W. Lu, T. Xu, Y. Wang, H. Hu, N. Li, X. Jiang and W. Chen, *Appl. Catal. B: Environ.*, 2016, **180**, 20–28.